

## Supplementary Information

### Fabrication of vulcanized cross-linked polystyrene grafted on carbon nanotubes for use as an advanced lithium host

Xian-lan Ke<sup>1</sup>, Yu-heng Lu<sup>1</sup>, Jin-lun Wu<sup>2,\*</sup>, Ding-cai Wu<sup>1,\*</sup>

(1. PCFM Lab, School of Chemistry, Sun Yat-sen University, Guangzhou, 510006, China

2. Guangdong Cardiovascular Institute, Guangdong Provincial People's Hospital, Guangdong Academy of Medical Sciences, Guangzhou, 510080, China)

Corresponding author: Jin-lun Wu, E-mail: [wujinlun@gdph.org.cn](mailto:wujinlun@gdph.org.cn);

Ding-cai Wu, E-mail: [wudc@mail.sysu.edu.cn](mailto:wudc@mail.sysu.edu.cn).

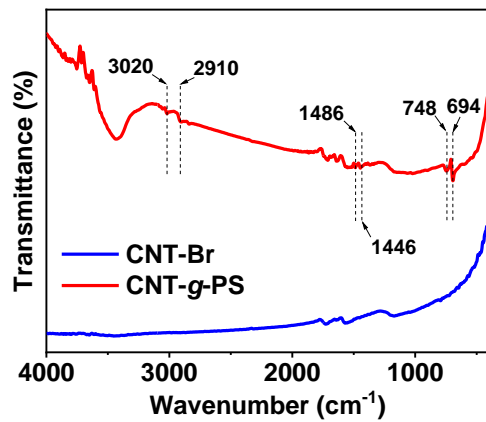


**Fig. S1** FTIR spectra of CNT-Br and CNT-g-PS.

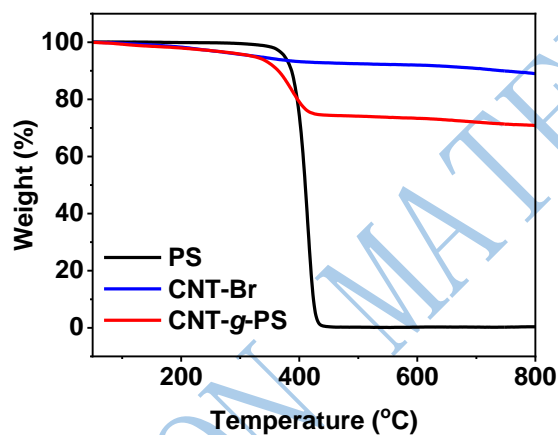


**Fig. S2** TGA curves of PS, CNT-Br, and CNT-g-PS.

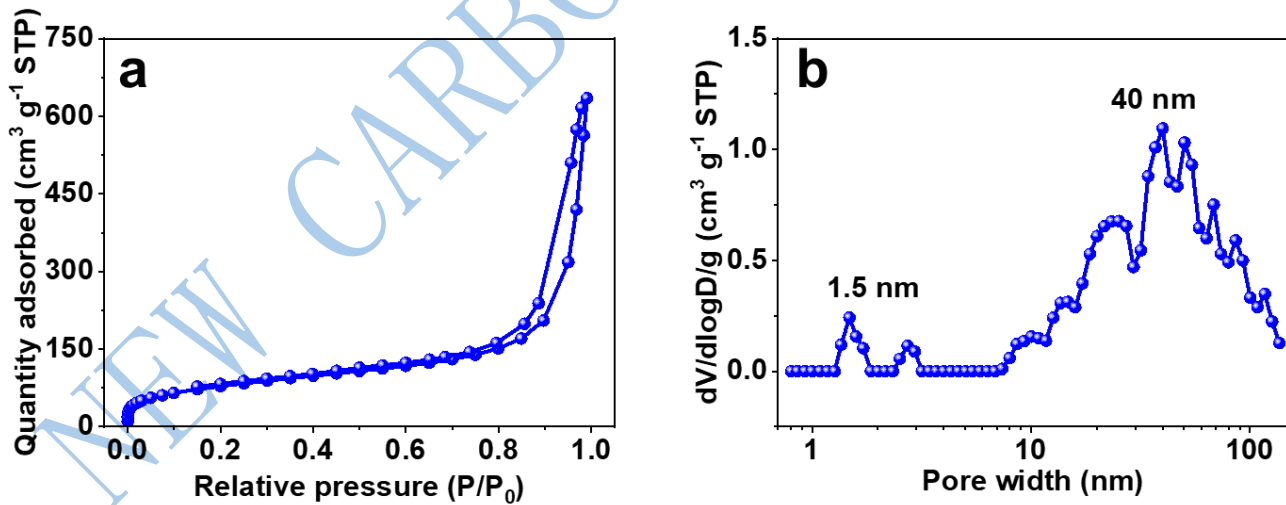


**Fig. S3** a) N<sub>2</sub> adsorption-desorption isotherm and b) DFT pore size distribution curves of CNT-g-xPS.

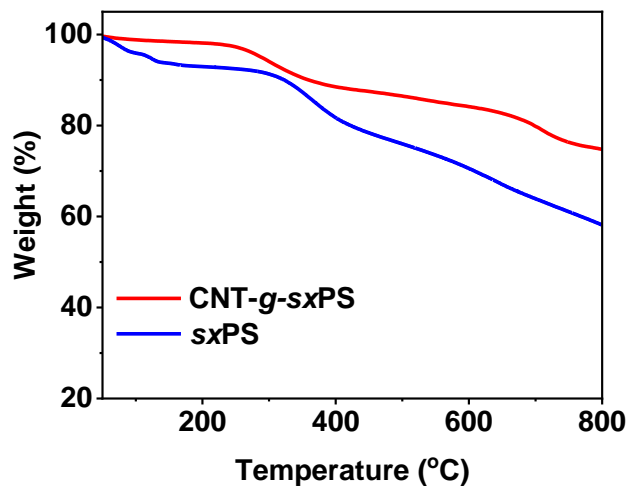


**Fig. S4** TGA curves of sxPS and CNT-g-sxPS.

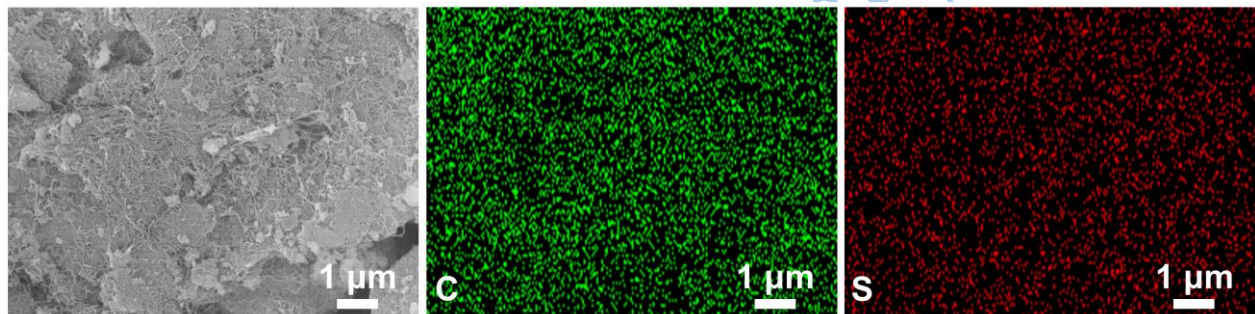


**Fig. S5** SEM image and corresponding elemental mapping images of CNT-g-sxPS.

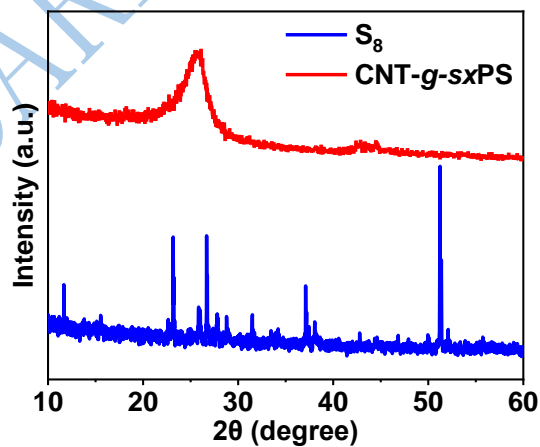


**Fig. S6** XRD patterns of S<sub>8</sub> and CNT-g-sxPS.

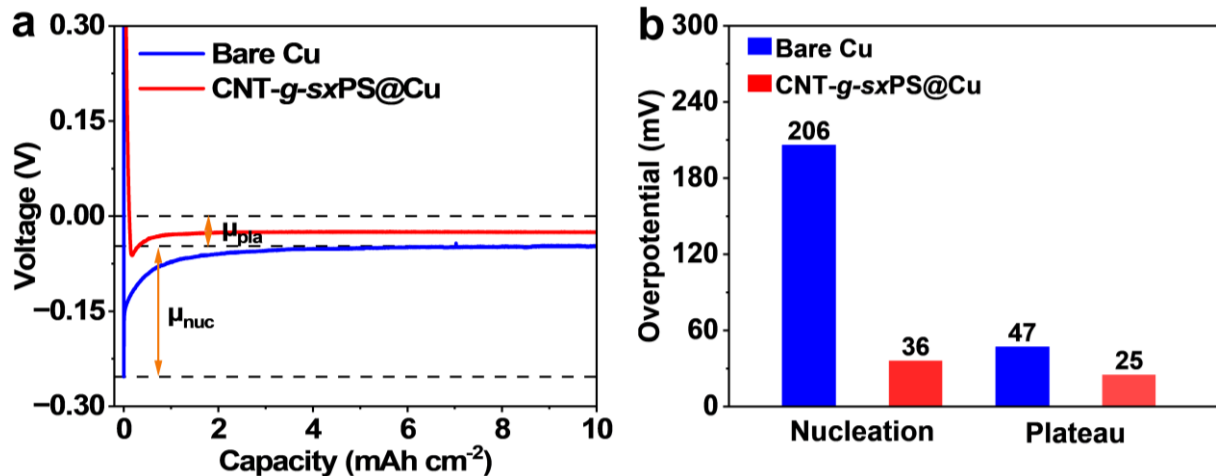


**Fig. S7** a) Voltage profiles of galvanostatic Li deposition and b) corresponding overpotentials on bare Cu and CNT-g-sxPS@Cu at a fixed current density of  $1 \text{ mA cm}^{-2}$ .

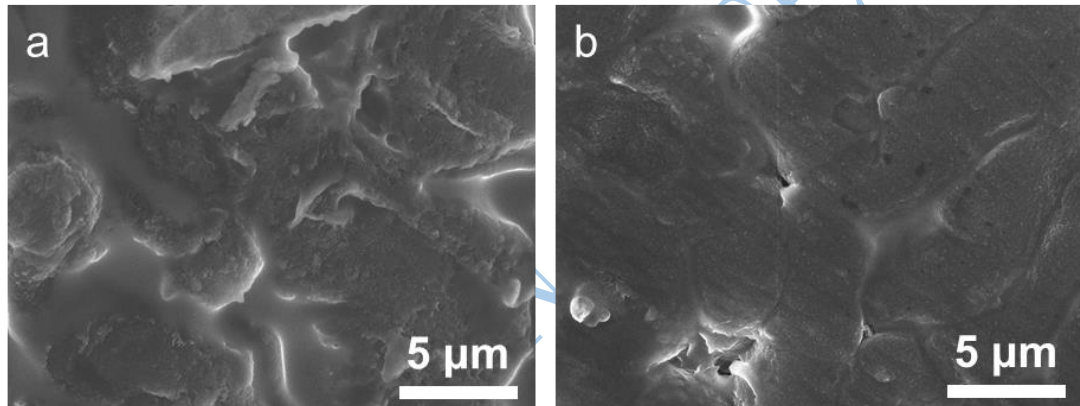


**Fig. S8** SEM images of a) bare Cu/Li and b) CNT-g-sxPS@Cu/Li.

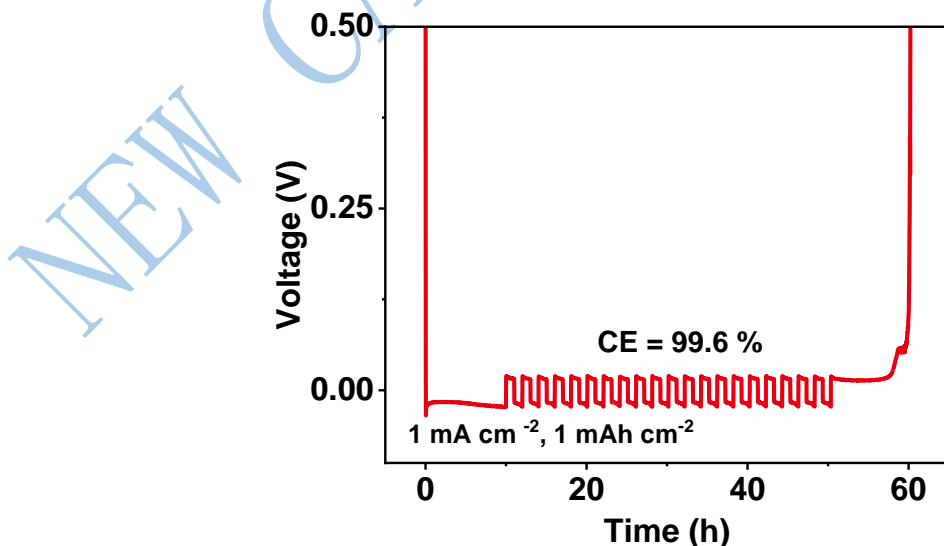


**Fig. S9** Coulombic efficiency of the cell with CNT-g-sxPS@Cu at  $1 \text{ mA cm}^{-2}$  and  $1 \text{ mAh cm}^{-2}$ .

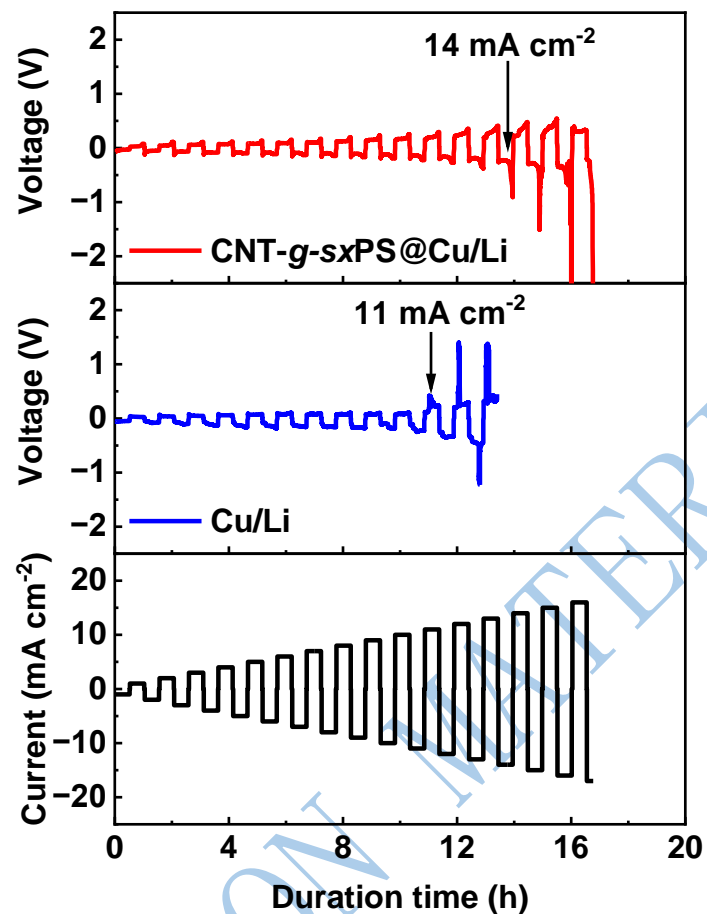


**Fig. S10** Voltage-time profiles for critical current density tests of Li|Li symmetric cells with CNT-g-sxPS@Cu/Li and bare Cu/Li anodes.

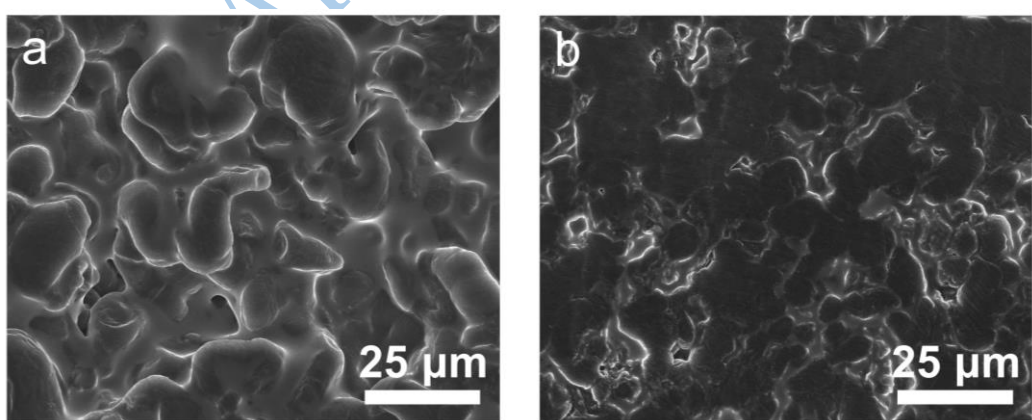


**Fig. S11** Top-view SEM images of a) bare Cu/Li and b) CNT-g-sxPS@Cu/Li anodes after Li|Li symmetric cell tests for 50 cycles at  $1 \text{ mA cm}^{-2}$  and  $1 \text{ mAh cm}^{-2}$ .

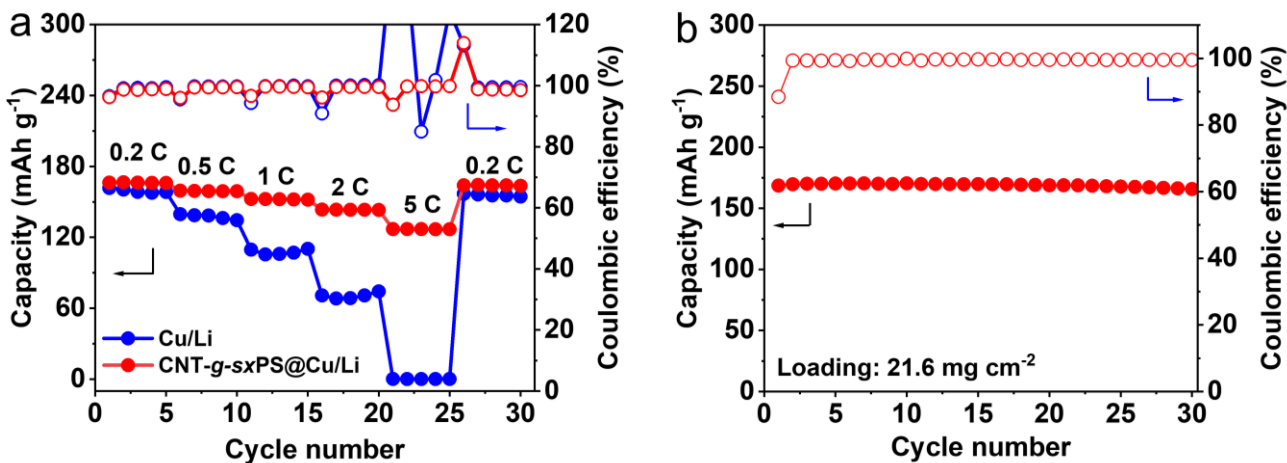


**Fig S12** a) Rate performance of the Li|NCM622 cells with bare Cu/Li and CNT-g-sxPS@Cu anodes.  
b) Cycling performance of the Li|NCM622 cell with CNT-g-sxPS@Cu anode at 0.1 C.

**Table S1.** Performance comparison of symmetric Li|Li cells with CNT-g-sxPS hosts to reported carbon-based hosts

Sample	Current density ( $\text{mA cm}^{-2}$ )	Areal capacity ( $\text{mAh cm}^{-2}$ )	Duration time (h)	Refs
CNT-g-sxPS@Cu/Li	1	1	500	This work
VG/CC	1	1	450	[1]
CF/Ag-Li	1	1	400	[2]
MOF-C(30)/Cu	0.4	0.4	500	[3]
Li@PCSF	2	1	100	[4]
Fe50	1	0.5	420	[5]
Li@CC	1	1	400	[6]
Li@HPTCF	1	1	300	[7]

#### References

- [1] Yan C, Xu T, Ma C, et al. Dendrite-free Li metal plating/stripping onto three-dimensional vertical-graphene@carbon-cloth host[J]. *Frontiers in Chemistry*, 2019, 7: 714.
- [2] Zhang R, Chen X, Shen X, et al. Coralloid carbon fiber-based composite lithium anode for robust lithium metal batteries [J]. *Joule*, 2018, 2(4): 764-777.
- [3] Yun J, Rim H, Won E, et al. Confined Li metal storage in porous carbon frameworks promoted by strong Li–substrate interaction[J]. *Chemical Engineering Journal*, 2022, 430: 132897.
- [4] Xue P, Sun C, Li H, et al. Superlithiophilic amorphous  $\text{SiO}_2\text{-TiO}_2$  distributed into porous carbon skeleton enabling uniform lithium deposition for stable lithium metal batteries[J]. *Advanced Science*, 2019, 6(18): 1900943.
- [5] Yu Z, Han D, Chen J, et al. In-situ growth of iron nanoparticles on porous carbon nanofibers for structural high-performance lithium metal anode[J]. *Electrochimica Acta*, 2022, 422: 140552.
- [6] Zhou Y, Han Y, Zhang H, et al. A carbon cloth-based lithium composite anode for high-performance lithium metal batteries [J]. *Energy Storage Materials*, 2018, 14: 222-229.
- [7] Cai W, Li G, Luo D, et al. The dual-play of 3D conductive scaffold embedded with Co, N codoped hollow polyhedra toward high-performance Li-S full cell[J]. *Advanced Energy Materials*, 2018, 8(34): 1802561.